

## Glider measurements around the Vercelli Seamount (Tyrrhenian Sea) in May 2009

E. MAURI, R. GERIN AND P.-M. POULAIN

*Istituto Nazionale di Oceanografia e di Geofisica Sperimentale - OGS, Trieste, Italy*

(Received: 22 December 2017; accepted: 2 April 2018)

**ABSTRACT** The Vercelli Seamount is an undersea topographic feature of the northern Tyrrhenian Sea which rises from around 2000 m depth to almost the surface (55 m depth). In late spring 2009 the interdisciplinary experiment “Tyrrhenian Seamounts Ecosystems: an integrated study” was conducted around the seamount to investigate its influence on the hydrodynamics and the biogeochemical conditions of the area. As part of this integrated study a Slocum glider was operated around the seamount from 23 to 30 May, 2009 to sample the physical and biogeochemical characteristics of the water column from the sea surface down to 190 m depth. The observations revealed little influence of the seamount on the near-surface circulation and water mass characteristics. They showed, however, slanted sub-mesoscale structures below the thermocline in the southern area of the seamount. These features evidenced in different recorded parameters are approximately compensated in density.

**Key words:** glider, Tyrrhenian Sea, Vercelli Seamount.

### 1. Introduction

The Tyrrhenian Sea is a Mediterranean sub-basin characterized by complex bottom topography: shallower in the north around 2000 m and deeper in the south over 3700 m. The northern basin communicates through the narrow (80 km) Corsica Channel with the Ligurian Sea and through a minor entrance, the Bonifacio Strait, separating Sardinia from Corsica, which connects it to the Liguro-Provençal basin. The complex topography of the basin is characterized by the presence of seamounts: the Vercelli Seamount in the north Tyrrhenian Sea off the Sardinia coast is one of them. It rises abruptly from the 2000 m seafloor and its summit is about 55 m below the surface, at about 41°05' N and 10°53' E (Fig. 1). The northern Tyrrhenian Sea is a very dynamical area, where several anticyclones and cyclones coexist (Artale *et al.*, 1994; Vetrano *et al.*, 2010); they can be induced by topographic effects (Vetrano *et al.*, 2010) or by wind-driven mechanisms (Nair *et al.*, 1994). The year-round westerly winds blowing through the Bonifacio Strait favour the presence of a permanent cyclonic gyre that characterises the area, called the Bonifacio gyre.

Independently of their origin, gyres contribute to the mixing and inflow of water masses of different types into the Tyrrhenian Sea. The cyclones generate vertical mixing, bringing nutrients from the intermediate waters to the euphotic zone. The uplifted water mass increases the local primary productivity as described in Morel and André (1991) and Nair *et al.* (1994). The

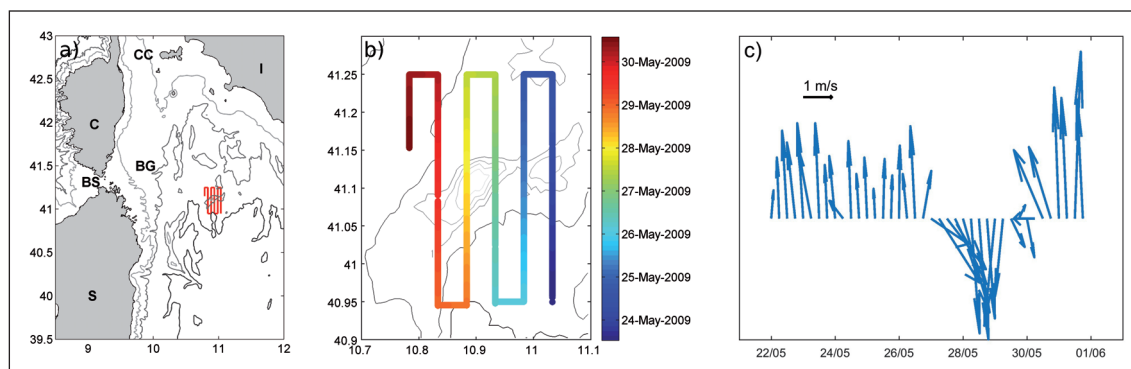


Fig. 1 - a) Tyrrhenian Sea sampling area. I: Italy, S: Sardinia, C: Corsica, BS: Bonifacio Strait, BG: Bonifacio Gyre, CC: Corsica Channel. The 200, 1000 and 2000 m isobaths are displayed in grey shades (from light to dark). The BG letters indicate the typical location of the gyre. b) Temporal evolution of the glider track overlaid on the bathymetry showing the Vercelli Seamount (bathymetry from Navionics). The deployment point is at the bottom right (23 May), while the recovery point is located at the top left (30 May). c) Vector diagram of the 6-hour Cross-Calibrated Multi Platform winds space-averaged on 12 grid points included in the area of study.

anticyclones, instead, are characterized in their inner core by oligotrophic conditions, as reported by Povero *et al.* (1990) and Astraldi and Gaparini (1994).

In this complex scenario, the “Tyrrhenian Seamounts ecosystems: an Integrated Study” (TySEc) experiment took place in late spring 2009 with the aim of studying the hydrodynamics of the area over and around the Vercelli Seamount. To better inquire about the effect of the seamount on the water mass biogeochemical and physical characteristics (e.g. the possible existence of a Taylor column over the seamount), a hydrographical cruise (14-day long) was conducted in an area of about  $80 \times 90$  km<sup>2</sup> surrounding the seamount. A glider campaign (8-day long) was carried on in a smaller area ( $20 \times 35$  km<sup>2</sup>) centred on the top of the seamount, to obtain measurements at a higher spatial resolution. The results of this glider campaign are presented in this paper.

From the analysis of the TySEc hydrographic cruise data only, Misic *et al.* (2012) tested the hypothesis of a bottom-trapped larval aggregation expected in a classical Taylor cap on an intermediate depth seamount. The authors concluded that, due to the complex hydrodynamic features in the area, a significant ‘seamount effect’ could not be found. Our study, based on higher spatial resolution glider data collected in a smaller area and during a shorter period, has the aim to inquire whether the glider data can provide a finer description at a smaller scale of the area under study and eventually provide new insights of the local hydrodynamics.

The paper is organized as follows: Section 2 presents the methods and introduces the data used to support the analysis, Section 3 describes the results divided in two main subsections: the evolution of the surface hydrological characteristics and the slanted features sampled in the southern part of the study area. The discussion and the conclusions are in Section 4.

## 2. Material and methods

Gliderers are autonomous underwater vehicles without propeller (Davis *et al.*, 2002; Rudnick *et al.*, 2004; Testor *et al.*, 2010). The glider used in this study is an electric coastal Slocum designed to work in littoral areas (down to 200 m depth). It is equipped with oceanographic sensors to measure

temperature, salinity: Sea-Bird Electronics SBE 41 CP CTD, oxygen: AANDERAA optode 3835, turbidity and chlorophyll: WET Labs - FLNTUS. The glider moves through the water column by changing its buoyancy; the wings convert part of the vertical movement into forward motion producing a saw-tooth pattern between the surface and the set depth. It reaches a vertical speed of 10-20 cm/s and a forward horizontal speed of about 20-40 cm/s. The glider is 1.5 m long with 20 cm diameter and it weighs about 50 kg in air. The two-way communication through the iridium satellite system occurs when the glider is at the surface. The underwater navigation follows a dead reckoning system using heading, pitch and roll recorded by the on-board sensors.

A dedicated glider campaign of about 8 days (from 23 to 30 May 2009) was organized as part of the TySEc experiment. The glider path followed a surface 'radiator' pattern covering an area of roughly 750 km<sup>2</sup> (20×35 km<sup>2</sup>) over the Vercelli Seamount (Fig. 1). Around 300 profiles, from the surface to 190 m depth, were acquired providing temperature, salinity, oxygen, fluorescence, and turbidity data. The glider was configured to provide scientific data only during the ascending phase providing a horizontal resolution of about 0.75 km. Some malfunctions of the fluorimeter and turbidity sensor were reported on 27-28 May and the corresponding erroneous data were flagged.

The collected data were interpolated to a grid of about 0.5 m in the vertical and 1 m horizontally and are represented in 3D to better depict the radiator shape glider route. The five shorter legs of the glider route (E-W transects) are omitted in the figures and only the 5 meridional longer (N-S) transects are plotted. The top of the seamount is located between the third and the fourth meridional transect (starting from the left) leaving the top of the seamount between the sample transects well above the 190 m depth reached by the glider (Fig. 1b). The shape of the seamount is not reported on the figure for sake of clarity.

Nightly sea surface temperature (SST) from advanced very high resolution radiometer (AVHRR) operating on NOAA near polar orbiting satellites, were processed for the period of the experiment. The multichannel sea surface temperature (MCSST) algorithm described by McClain *et al.* (1985) was used to compute SST. Temperature images at 1 km ground resolution were created for the northern Tyrrhenian Sea.

The products from the cross-calibrated multi platform (CCMP) dataset were used to characterise the wind regime of the study area during the period of the glider experiment. The CCMP data set combines cross-calibrated satellite winds obtained from remote sensing systems using a variational analysis method to provide 6-hourly wind speed and direction on a high-resolution (0.25 degree) grid (Atlas *et al.*, 2009). Wind data were downloaded and space-averaged over the 12 grid points included in the area of study.

The sea level anomaly (SLA) data used for this study are the gridded (1/8° Mercator projection grid) Ssalto/Duacs daily, multi-mission, delayed time (quality controlled) products from AVISO (Pujol *et al.*, 2016; Ssalto/Duacs User Handbook, 2016), downloaded for the period May 2009.

### 3. Results

#### 3.1. Surface layer

A sequence of SST images during the period of the experiment shows the evolution of the surface water masses in the northern Tyrrhenian Sea. The area of the study (black square in Fig. 2) was characterised by an almost homogenous warm layer (about 22.5° C) on 25 May

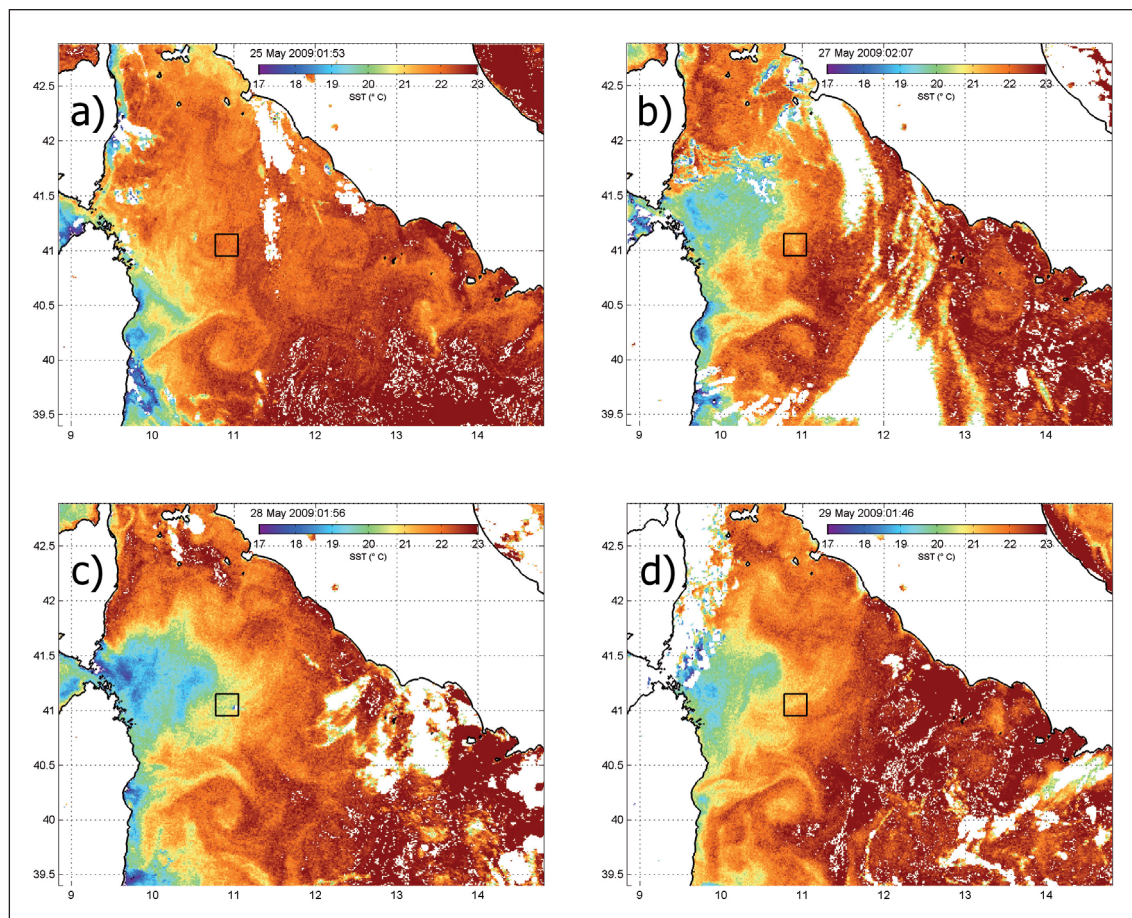


Fig. 2 - Nightly SST satellite images for the 25, 27, 28, and 29 May. The black square indicates the area of the experiment occurred between 23 May and 3 June. Same colour scale is applied; the limits are 17-23° C.

(Fig. 2a). Starting from 27 May (Fig. 2b) the surface temperature became cooler between Corsica and Sardinia due to the ingression of a colder water mass coming from the Bonifacio Strait. In the early morning of 28 May (Fig. 2c) the area of study was affected by the above mentioned cooling and the surface temperature reached about 20° C.

The wind intensity and direction during the glider campaign are presented in Fig. 1c. At the beginning of the experiment, the wind blew from the south with maximum speed of 3 m/s. Starting from 27 May the wind changed direction to blow from NW with a slightly higher speed and lasting for the next two days.

The glider temperature data (Fig. 3a) revealed a shallow (5-10 m deep) mixed layer with maximum temperature of 23° C present in the easternmost two transects, i.e. from the beginning of the campaign until 27 May (central transect). The positions of the glider at specific times are presented in Fig. 1b. In the second part of the campaign, the temperature at the surface suddenly decreased to less than 21° C and the mixed layer deepened to more than 15 m. A slight increase of the surface temperature was recorded on 28 May. The salinity (Fig. 3b) varied between a minimum around 37.85 and a maximum of 38.25 in the top 20 m layer before 27 May probably in coincidence with the slanted mesoscale features seen in the deeper layers, discussed below.



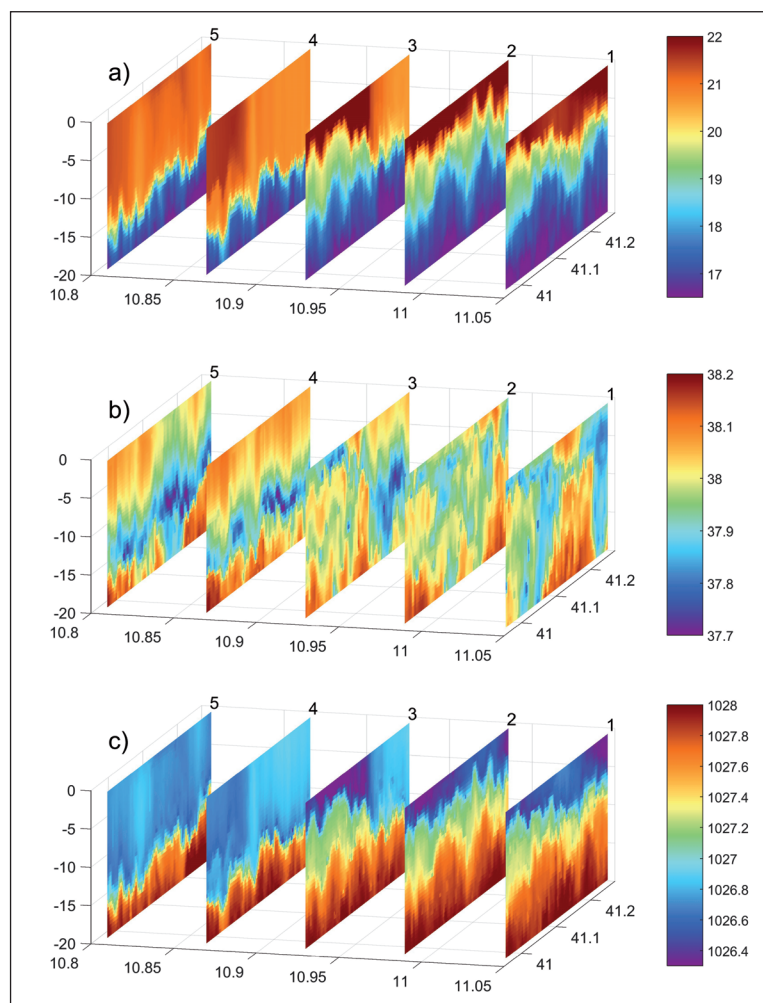


Fig. 3 - Temperature °C (a), salinity (b) and density ( $\text{kg/m}^3$ ) (c) in the first 20 m during the entire mission. X label is longitude and Y label is latitude. Transect numbers from east to west, i.e. chronologically are posted on top of each plot. The top of the seamount is located between the third and the fourth meridional transects (Fig. 1b).

After 27 May, the salinity became more homogeneous in the top 10 m. Lighter water masses with density of  $1026.5 \text{ kg/m}^3$  in the first 5 m layer became denser after 27 May, reaching  $1026.9 \text{ kg/m}^3$  in the top 15 m layer (Fig. 3c).

### 3.2. Layer below the mixed layer from 60 to 190 m

Although the layer below 60 m seems not to be affected by the change in meteorological conditions, all the measured parameters showed mesoscale and sub-mesoscale variability (Figs. 4 and 5). A sharp gradient was present in this deeper layer, around  $41.15^\circ \text{N}$ ; north of it the temperature and salinity were respectively around  $15.5^\circ \text{C}$  and  $38.6$  (Figs. 4a and 4b) while oxygen concentration was about  $220 \mu\text{M}$  (Fig. 5a), whereas south of  $41.15^\circ \text{N}$ , the temperature and salinity were lower and oxygen concentration was higher than in the northern area. The density did not show the same gradient (Fig. 4c), an increase of density with respect of the depth was evident in all transects.

The deep chlorophyll maximum (DCM) was located around 80 m following the base of oxygen maximum, from there, tongues of slightly higher chlorophyll reached 140 m (Fig. 5b). Some

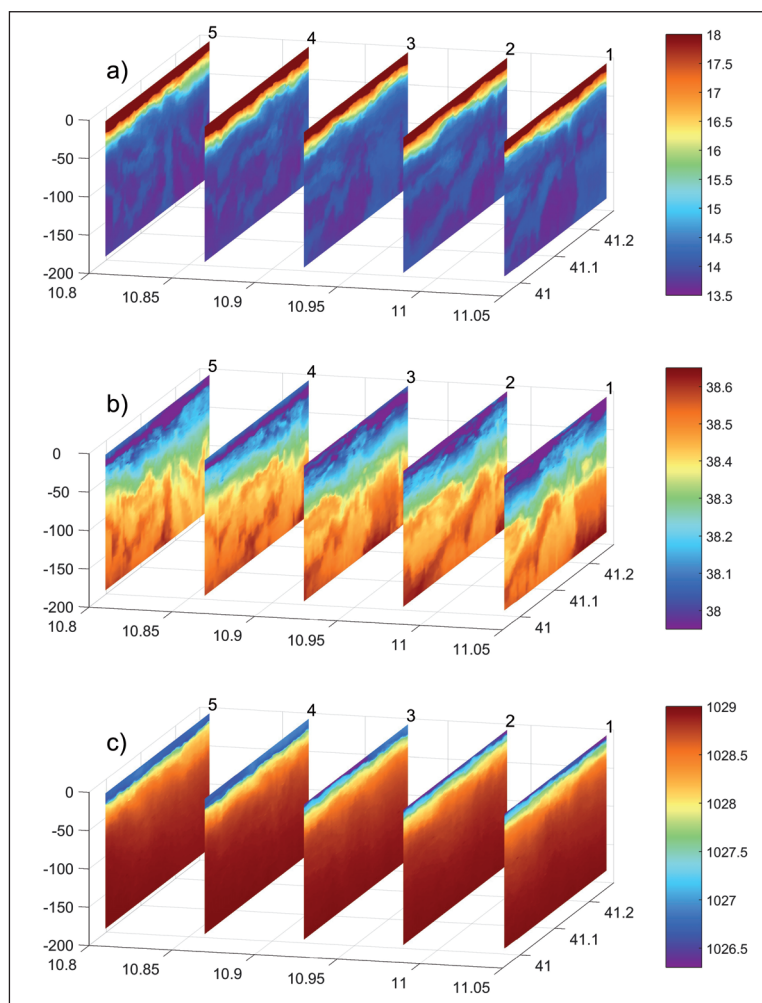


Fig. 4 - Temperature (a), salinity (b) and density (c) in the top 190 m during the entire mission. X label is longitude and Y label is latitude. Transect numbers from east to west, i.e. chronologically are posted on top of each plot. The top of the seamount is located between the third and the fourth meridional transects (Fig. 1b).

higher chlorophyll concentration patches along the DCM were located SW of the Vercelli summit on 28 May (transect 4 in Fig. 5b). North of it, the DCM is not well visible due to malfunction of the optical sensor. The turbidity showed the same patterns than chlorophyll with a maximum in the DCM and slightly higher values in the top layer. The sharp gradient seen in temperature, salinity and oxygen was also highlighted by higher turbidity values.

Slanted mesoscale features occurred in the southern portion of the sampled area. They became evident at 100 m depth extending down to 190 m, in the glider data. Their meridional extension was about 10-15 km. In the zonal direction, they occurred coherently at least over 28 km. Indeed in the first four sections the structures had the same inclination around 6 degrees from the sea surface, while in the last section the structures were less coherent with the previous sections. These features were characterized by lower oxygen concentration, higher temperature, salinity and chlorophyll values, compared to the surrounding waters; the differences were respectively of 40  $\mu\text{M}$ , 0.8° C, 0.1 0.5  $\text{mg}/\text{m}^3$ , respectively. The inclined upper margin was marked not only by higher chlorophyll concentration but also by higher turbidity.

The general circulation of the northern Tyrrhenian Sea was investigated, analysing the 5-day

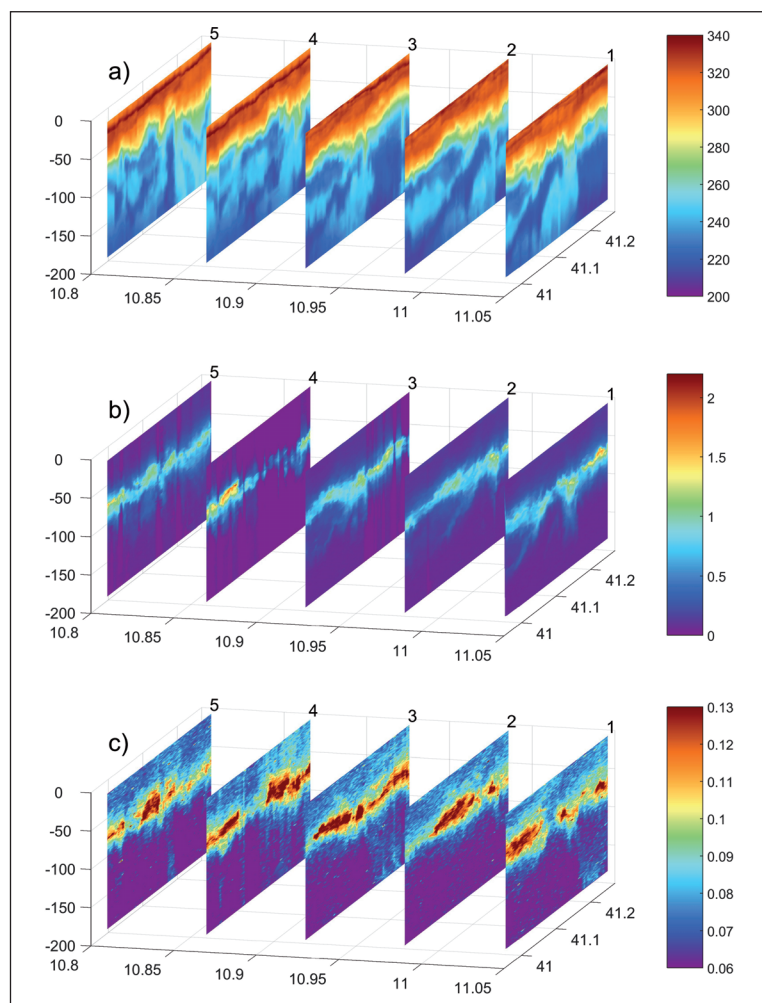


Fig. 5 - Oxygen concentration ( $\mu\text{M}$ ) (a), chlorophyll concentration ( $\text{mg}/\text{m}^3$ ) (b), turbidity (NTU) (c) in the top 190 m during the entire mission. X label is longitude and Y label is latitude. Transect numbers from east to west, i.e. chronologically are posted on top of each plot. The top of the seamount is located between the third and the fourth meridional transects (Fig. 1b).

averaged SLA centred on 27 May (Fig. 6). A transition zone between a cyclone to the south and an anticyclone to the north characterized the area under study.

#### 4. Discussion and conclusions

Glider data have been recorded in the central Tyrrhenian Sea (western Mediterranean Sea), on a 5-transect pattern covering the Vercelli Seamount, which sharply rise up to 55 m depth from 2000 m seafloor. The data reveal a stratified condition of the top 5 m layer evolving during the experiment, to a deeper mixed layer reaching 15 m with higher temperature and density. After 27 May the surface water characteristics are the result of the vertical mixing between the local surface water and the water advected from the Bonifacio Strait. The intruded water, characterized by high salinity and low oxygen concentration, probably originates from the wind-induced upwelling which occurred west and inside the Bonifacio Strait. The uplifted waters are pushed through the strait and reach the area of the seamount in a few days as shown by the SST images.

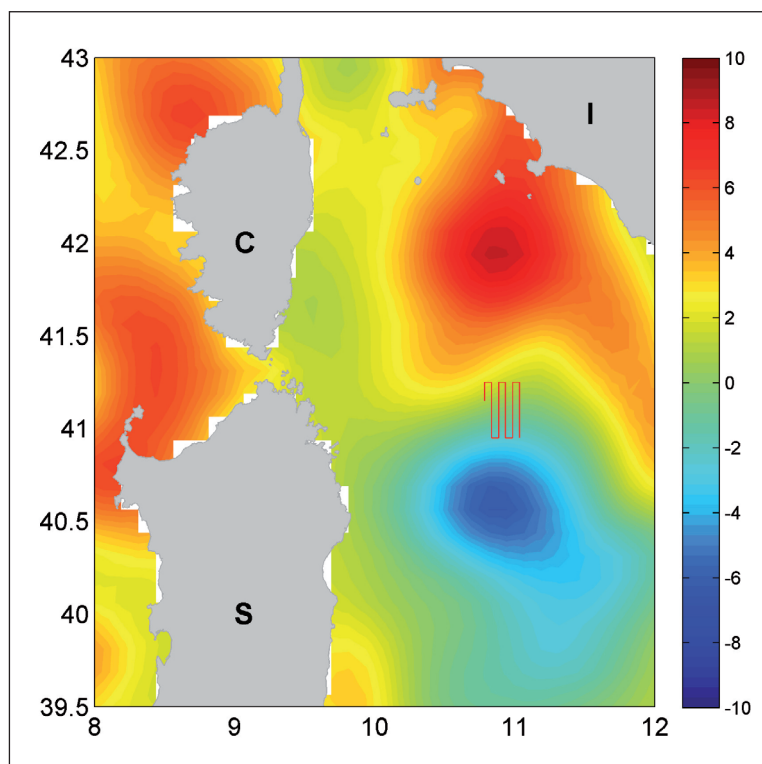


Fig. 6 - Five-day averaged SLA centred on 27 May of the northern Tyrrhenian Sea. Values are reported in cm.

The weak Mistral event around 27 May, in the middle of the glider campaign, perturbs a stable stratification hiding the potential seamount effect of the Vercelli summit on the surface layer.

The layer below the mixing depth, not affected by the changing atmospheric conditions, highlights a front at around 41.15° N and slanted features in the southern area around the seamount. The front corresponds to variations of almost 1° C in temperature, by one tenth in salinity and 40  $\mu\text{M}$  in oxygen concentration. Warmer, saltier and less oxygenated waters than in the surrounding areas characterize the slanted structures, visible in all the parameters. The concentration differences across the features are similar to those of the front. The optical parameters, like chlorophyll concentration and turbidity, which are low in the above features and north of the front, emphasize the top margin of the features and the south part of the front, where the oxygen is relatively higher. It is worth noticing that the maximum chlorophyll and turbidity values are located around 80 m depth and only some inclined filaments are detached from this layer reaching 140 m. The vertical distribution of chlorophyll displays a pronounced maximum close to the base of the euphotic zone (Mignot *et al.*, 2011). Below this zone there is no more production, indicating a probable subduction mechanism.

Similar submesoscale features with high chlorophyll and oxygen concentration have been observed in a frontal zone between the Mediterranean and the Atlantic water in the Alboran Sea (Ruiz *et al.*, 2009). The tongue described by Ruiz *et al.* (2009) coincides with a density frontal zone, defined by temperature and salinity, suggesting the subduction of the water from the dense side of the front, below the frontal structure. Combining altimetry data and glider data the authors computed a considerable vertical motion of about 1 m/day. In our case, even if the structures are visible in



temperature and salinity, they are approximately compensated in density. In Niewiadomska *et al.* (2008) in the Ligurian Current, in well established frontal zones, a down-welled water flow was described, and the observed tongue was nearly isopycnal, similarly to our case in which the density is horizontally homogeneous. Even though there is no density signature showing a clear mesoscale structure, the SLA images indicate the presence of a cyclone to the south of the seamount summit. The chlorophyll slanted features indicate the presence of a down-welling mechanism occurring along the northern edge of the cyclone. The external area of a cyclone is classically described as a location of subduction mechanisms. In our measurements a first tongue detaching at 41.15° N and a second one from 41.10° N (at 11.04° E, at different longitudes the detaching position are slightly north or south) are observed but the mechanism driving their existence cannot be explained from the data collected. Such features open new questions on the role of the submesoscale eddies on the mixing/export mechanisms in the area of study.

A deeper investigation would be beneficial since the glider measurements show deep chlorophyll maximum (DCM) around 80 m depth with chlorophyll concentration of about 0.8 mg/m<sup>3</sup> with some higher chlorophyll patches, consistent with those measured by Misic *et al.* (2012). In the latter study, there are some findings that suggest an up-welling mechanism evidenced by higher nitrate, nitrite and phosphate only SE of the seamount or by the 10 km patch of high chlorophyll concentration sampled over the seamount summit. In our study, this increase of chlorophyll was detected only partially, slightly to the SW of the seamount. There is probably a combination of down and up welling mechanisms but they are insufficiently sampled.

In summary, the results obtained during the glider campaign, show a surface stratified layer highly influenced by local meteorological condition and a subsurface layer, below 80 m depth, characterized by submesoscale slanted features and fronts less affected by the weather conditions. The high resolution glider measurements allow identifying submesoscale features (e.g. slanted tongues) associated with a down-welling mechanism highlighted by higher chlorophyll concentration below the euphotic zone. The local hydrodynamics can certainly affect the ecosystem and consequently its biological component and have an important effect on the local redistribution of heat, salt and nutrients. However from the glider data alone, the seamount effect is difficult to be identified. The Vercelli Seamount can, eventually, have a topographic effect in constraining semi-permanent or permanent eddies as stated in Vetrano *et al.* (2010). A fleet of gliders operated simultaneously in a wider area would better resolve the synoptic condition of the area and provide more quantitative physical and biogeochemical data on the local dynamics.

**Acknowledgments.** We thank our colleagues A. Bubbi, F. Brunetti, N. Medeot, R. Nair for helping with the glider deployment and the piloting and the R/V Urania captain and crew for their assistance. Thanks to M. Menna for helping us with the SLA data.

#### References

- Artale V., Astraldi M., Buffoni G. and Gasparini G.P.; 1994: *Seasonal variability of gyre-scale circulation in the northern Tyrrhenian Sea*. J. Geophys. Res., **99**, 14127-14137.
- Astraldi M. and Gasparini G.P.; 1994: *The seasonal characteristics of the circulation in the Tyrrhenian Sea*. Coastal Estuarine Stud., **46**, 115-134.
- Atlas R., Ardizzone J.V., Hoffman R., Jusem J.C. and Leidner S.M.; 2009: *Cross-calibrated, multi-platform ocean surface wind velocity product (MEASUREs Project)*. Physical Oceanography Distributed Active Archive Center (PO.DAAC), JPL, Pasadena, CA, USA, Guide Document, Version 1.0, 26 pp.

- Davis R., Eriksen C. and Jones C.; 2002: *Autonomous buoyancy-driven underwater gliders*. In: Griffiths G. (ed), Technology and applications of autonomous underwater vehicles, Taylor and Francis, London, England, pp. 37-58.
- McClain E.P., Pichel W. and Walton C.; 1985: *Comparative performance of the AVHRR-based multichannel sea surface temperature*. J. Geophys. Res., **90**, 11587 - 11601, doi:10.1029/JC090iC06p11587.
- Mignot A., Claustre H., D'Ortenzio F., Xing X., Poteau A. and Ras J.; 2011: *From the shape of the vertical profile of in vivo fluorescence to Chlorophyll-a concentration*. Biogeosci., **8**, 2391-2406, doi:10.5194/bg-8-2391-2011.
- Misic C., Bavestrello G., Bo M., Borghini M., Castellano M., Covazzi Harriague A., Massa F., Spotorno F. and Povero P.; 2012: *The "seamount effect" as revealed by organic matter dynamics around a shallow seamount in the Tyrrhenian Sea (Vercelli Seamount, western Mediterranean)*. Deep Sea Res. Part I, **67**, 1-11.
- Morel A. and Andre' J.M.; 1991: *Pigment distribution and primary production in the western Mediterranean as derived and modelled from coastal zone color scanner observations*. J. Geophys. Res., **96**, 12685-12698.
- Nair R., Cattini E., Gasparini G.P. and Rossi G.; 1994: *Circolazione ciclonica e distribuzione dei nutrienti nel Tirreno settentrionale*. In: Proc. X Symp. Ital. Assoc. Limnol. and Oceanol. (AIOL), pp. 65-76.
- Niewiadomska K., Claustre H., Prieur L. and d'Ortenzio F.; 2008: *Submesoscale physical biogeochemical coupling across the Ligurian Current (northwestern Mediterranean) using a biooptical glider*. Limnol. Oceanogr., **53**, 2210-2225.
- Povero P., Hopkins T.S. and Fabiano M.; 1990: *Oxygen and nutrient observations in the southern Tyrrhenian Sea*. Oceanol. Acta, **13**, 299-305.
- Pujol M.-I., Faugère Y., Taburet G., Dupuy S., Pelloquin C., Ablain M. and Picot N.; 2016: *DUACS DT2014: the new multi-mission altimeter data set reprocessed over 20 years*. Ocean Sci., **12**, 1067-1090, doi:10.5194/os-12-1067-2016.
- Rudnick D., Davis R., Eriksen C., Fantantoni D. and Perry M.J.; 2004: *Underwater Gliders for ocean research*. Mar. Technol. Soc. J., **38**, 48-59.
- Ruiz S., Pascual A., Garau B., Pujol I. and Tintoré J.; 2009: *Vertical motion in the upper-ocean from glider and altimetry data*. Geophys. Res. Lett., L14607, doi:10.1029/2009GL03856.
- Ssalto/Duacs User Handbook; 2016: (M)SLA and (M)ADT Near-Real Time and Delayed Time Products, CLS-DOS-NT-06-034.
- Testor P., Meyers G., Pattiaratchi C., Bachmayer R., Hayes D., Pouliquen S., Petit de la Villeon L., Carval T., Ganachaud A., Gourdeau L., Mortier L., Claustre H., Taillandier V., Lherminier P., Terre T., Visbeck M., Karstensen J., Krahnemann G., Alvarez A., Rixen M., Poulain P.-M., Osterhus S., Tintore J., Ruiz S., Garau B., Smeed D., Griffiths G., Merckelbach L., Sherwin T., Schmid C., Barth J.A., Schofield O., Glenn S., Kohut J., Perry M.J., Eriksen C., Send U., Davis R., Rudnick D., Sherman J., Jones C., Webb D., Lee C. and Owens B.; 2010: *Gliders as a component of future observing systems*. In: Proc. OceanObs'09, Hall J., Harrison D.E. and Stammer D. (eds), Sustained Ocean Observations and Information for Society (Vol. 2), Venezia, Italy, ESA Publication WPP-306, doi:10.5270/OceanObs09.cwp.89.
- Vetrano A., Napolitano E., Iacono R., Schroeder K. and Gasparini G.-P.; 2010: *Tyrrhenian Sea circulation and water mass fluxes in spring 2004: observations and model results*. J. Geophys. Res., **115**, C06023, doi:10.1029/2009JC005680.

Corresponding author: Elena Mauri  
Istituto Nazionale di Oceanografia e di Geofisica Sperimentale (OGS)  
Borgo Grotta Gigante 42/c, 34010 Sgonico, Trieste  
Phone: +39 040 2140203; e-mail: emauri@inogs.it